



1 Benthic foraminiferal species tolerance for hydrothermal activity: a case of study from the  
2 Lucky Strike vent field.

3 Pierre-Antoine Dessandier<sup>1</sup>, Giuliana Panieri<sup>2</sup>, Riwan Leroux<sup>1</sup>, Ewan Pelleter<sup>3</sup>, Sandra Fuchs<sup>1</sup>,  
4 Alizé Bouriat<sup>1</sup>, Audrey Boissier<sup>3</sup>, Sandrine Cheron<sup>3</sup>, Jozée Sarrazin<sup>1</sup>

5

6 1 Univ Brest, Ifremer, BEEP, F-29280 Plouzané, France

7 2 Department of Geosciences, UiT - The Arctic University of Norway, 9037, Tromsø, Norway

8 3 Geo-Ocean, University Brest, CNRS, Ifremer, UMR6538, Plouzane, France

9 Corresponding author: Pierre-Antoine Dessandier, [pierre.antoine.dessandier@ifremer.fr](mailto:pierre.antoine.dessandier@ifremer.fr)

10

11 Abstract

12 Hydrothermal vent fields represent dynamic environments hosting rich ecosystems. At the Mid-  
13 Atlantic Ridge, the Lucky Strike (LS) vent field has been the focus of multiple biological  
14 studies. While ecological studies have been focusing on microbial and macrofaunal  
15 communities, some groups still remained out of the scope. We present here the first ecological  
16 study of benthic foraminifera inhabiting soft sediments in the peripheries of hydrothermal  
17 edifices at LS. A total of fifteen blade cores were analyzed. We combine microhabitat  
18 environmental descriptors with faunal density and diversity of benthic foraminifera (living &  
19 fossil) to investigate the impact of hydrothermal activity on their ecology. The far periphery,  
20 ~150 m away from vents, harbors a community of diverse foraminifera feeding on pre-degraded  
21 organic matter characterized by a phytoplankton detrital signal. Communities located at  
22 intermediate distance (~ 50 m) from venting showed the presence of opportunistic species likely  
23 feeding on chemosynthetic microorganisms. Finally, environments closer to active sites (few



24 meters) showed very low abundance of living individuals, as the presence of harsh  
25 environmental conditions may limit foraminiferal growth. Unexpectedly, the presence of  
26 widespread iron-oxidizer bacterial biofilms was associated to the dissolution of all biogenic  
27 carbonate content raising questions on their impact on regional carbon budget.

28 Key words: Benthic foraminifera, hydrothermal activity, Lucky Strike vent filed, microbial  
29 biofilm.

30

31 1. Introduction

32 Benthic foraminifera are marine micro-organisms that represent more than 50% of the  
33 eukaryotic biomass in many deep-sea habitats and influence the structure and dynamics of  
34 marine biological communities, with benthic organisms as predators and microorganisms as  
35 preys (Gooday et al., 1994). These organisms have been widely studied as fossils in marine  
36 systems for more than a century and as living individuals for ecological purpose over the last  
37 decades. However, very few studies have been conducted on benthic foraminifera from deep-  
38 sea hydrothermal vents (Molina-Cruz and Ayala-Lopez, 1988; Jonasson et al., 1995; Burkett et  
39 al., 2018; Krüger et al., 2025) because of complex sampling techniques (hard substrates) and  
40 the usual focus on microbes and macrofauna in these environments.

41 Benthic foraminiferal distribution in the marine sediment is mainly controlled by the spatially  
42 opposed contents of organic matter and oxygen (Jorissen et al., 1995), but also by organic matter  
43 quality and source (e.g., Dessandier et al., 2016). In deep-sea environments, the food source for  
44 benthic foraminifera is often limited to degraded detrital material and microbial organic matter  
45 (Gooday et al., 1992). In extreme environments, where fluids enhance microbial activities,  
46 benthic foraminifera can thrive feeding on certain groups of bacteria, where the conditions  
47 allow them to survive (Dessandier et al., 2019).



48 Extreme environments thus offer a nutrient-rich microbial food source for benthic foraminifera,  
49 yet they also represent a potentially harsh environment due to their challenging physical and  
50 chemical conditions. Hydrothermal vents are dynamic systems where cold seawater penetrate  
51 through cracks in the ocean crust and is heated and enriched in dissolved metals and sulfur in  
52 contact with rocks overlying the magma chamber. This process results in the emergence of hot,  
53 slightly acidic and chemically reduced fluids. Most of the metals dissolved in the ascending  
54 vent fluids precipitate when they mix with the surrounding cold seawater, resulting in black-  
55 and white smoker chimneys, large sulfide edifices and later, extensive mounds of accumulated  
56 massive sulfide. Hydrothermal vent fields are commonly referred as to “oases of life”,  
57 harboring luxuriant endemic chemosynthetic faunal communities (Fisher et al., 2007).  
58 Associated food webs are mainly based on local microbial chemosynthesis (Childress and  
59 Fisher, 1992), performed by free-living and symbiotic chemoautotrophic microorganisms that  
60 utilize the chemical energy released by the oxidation of reduced chemicals species ( $H_2$ ,  $H_2S$ ,  
61  $CH_4$ , Fe) present in the hydrothermal fluids (Childress and Fisher, 1992, Schmidt et al. 2008).  
62 In Juan de Fuca Ridge (North Pacific Ocean), the distribution of foraminifera was shown to be  
63 influenced by temperature, pH and substratum types, resulting in their absence at temperature  
64 higher than 20°C and on unstable surfaces such as friable anhydrite which prevents the  
65 attachment of agglutinated species (Jonasson et al., 1995). Among hydrothermal vent systems,  
66 the Lucky Strike vent field has been one of the most studied ecosystems since its discovery in  
67 1992 and with more than 15 years of continuous multidisciplinary observations through the  
68 EMSO-Azores observatory deployed in 2010 (Matabos et al., 2025). Over these studies, it has  
69 been pointed out that regional distributions of macro- and meiofauna depend on abiotic  
70 parameters such as pH, temperature, sulfides and metals (e.g., Sarrazin et al., 2015, see Matabos  
71 et al., 2025 for a review). However, no studies yet filled the gaps about the role of the  
72 foraminiferal compartment in this system. Given its numerous active vent sites and well

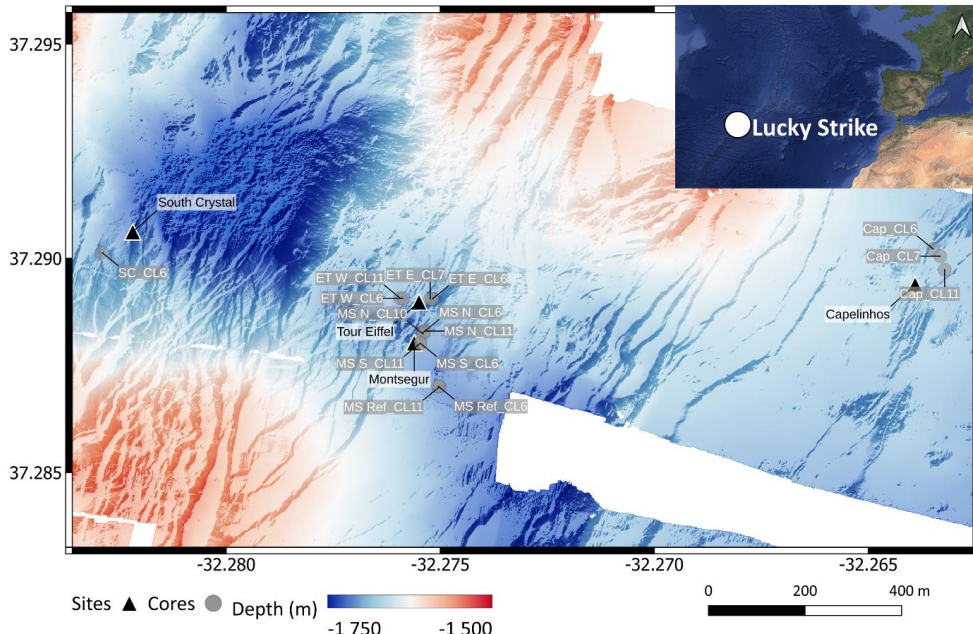


73 documented biotic and abiotic conditions, the Lucky Strike vent field provides an ideal setting  
74 for investigating benthic foraminiferal ecology in hydrothermal ecosystems and their role in  
75 influencing regional biodiversity. This study presents the first analysis of benthic foraminifera  
76 from the Lucky Strike vent field, integrating living and fossil foraminiferal individuals and  
77 environmental conditions across gradients of hydrothermal influence and associated microbial  
78 biofilms.

79

80 2. Study area

81 The Lucky Strike hydrothermal vent field on the Mid-Atlantic Ridge (MAR) at 37°17'N is one  
82 of the largest fields. It is located at ~1,700 m water depth and its ~25 active edifices are  
83 surrounding a 200 m diameter lava lake (Ondréas et al., 2009). Biological and geological  
84 evidence indicate a long venting history at Lucky Strike, with recent lava footprint analyses  
85 suggesting that modern volcanic activity has driven the resurgence of hydrothermal venting  
86 (Langmuir et al., 1997). Several active and inactive edifices have been identified since the first  
87 exploration of the field in 1993 (Fouquet et al., 1995). In addition to the sulfide structures, the  
88 seafloor is characterized by sulfide deposits and covered by hydrothermal slab corresponding  
89 to breccia of basaltic glass and plagioclase crystals indurated by silica and barite (Langmuir et  
90 al., 1997). The sediments surrounding the structures contain high concentration of metals such  
91 as Fe, Cu and Zn, particularly enriched at the Capelinhos vent site where the fault configuration  
92 enables hot fluid outflow (>300°C) (Fig. 1, Cotte et al., 2020).



93

94 Fig. 1. Location of the Lucky Strike vent field on the Mid-Atlantic Ridge (inset) and of the  
95 sediment cores (grey circles) collected in 2020 near four active hydrothermal edifices (black  
96 triangle).

97

98 As observed in many different hydrothermal fields, the local biology is greatly enhanced by  
99 symbiosis with chemosynthetic microorganisms. That results at Lucky Strike in a strong  
100 dominance of *Bathymodiolus azoricus* mussel assemblages (Van Dover, 1995; Desbruyeres et  
101 al., 2001) that create habitats hosting at least 79 associated species, each occupying distinct  
102 ecological niches (Sarrazin et al., 2015; Husson et al., 2017; Sarrazin et al., 2020). Two other  
103 assemblages, dominated respectively by *Mirocaris fortunata* shrimp and by *Peltospira*  
104 *smaragdina* gastropods, dominate warmer areas (Sarrazin et al., 2022). The geochemistry of  
105 the plumes showed a strong dilution of the fluid a few meters (5 to 10 m) away from the venting  
106 locations, as suggested by measurements of temperature and pH gradients near one of the  
107 largest and most studied edifices (i.e., Eiffel Tower; Sarradin et al., 2009). The area of exported



108 particles does not reach 500 m and the influence of the vent field on the open ocean remains  
109 restricted (Khripounoff et al., 2000). Even though the Lucky Strike vent field differs from the  
110 other Mid-Atlantic Ridge vent sites by the absence of well-developed peripheral macrofauna  
111 (Van Dover et al., 1996), the vent primary chemosynthetic production is exported at least as far  
112 as ~90 m in the field (Alfaro-Lucas et al., 2020). The peripheral fauna harbors unique species  
113 and functional entities that contribute to increase the biodiversity at the vent field scale (Alfaro-  
114 Lucas et al., 2020).

115

### 116 3. Material and methods

117 During the MoMARSAT cruise in September 2020, 15 sediment blade cores have been  
118 collected using the remotely operated vehicle *Victor6000* (Ifremer, Fig.1). Among them, 1 core  
119 was not analyzed due to missing sedimentary material, and 3 of them targeted microbial mats,  
120 visually attributed to iron-oxidizers biofilms, most likely zetaproteobacteria (Astorch-Cardona  
121 et al., 2023). Various venting locations were targeted (i.e., near Eiffel Tower, Montsegur,  
122 Capelinhos and South Crystal edifices) in addition to a more distal location ~100 m away from  
123 active venting (called Montsegur-Ref, Fig. 1). Each core has been sliced on board every  
124 centimeter and split in two equivalent volumes for each horizon, one preserved at -20°C for  
125 geochemical analyses and one preserved in a solution of Rose Bengal 2 g L<sup>-1</sup> in 96% ethanol  
126 for living benthic foraminiferal identification (Table 1). The taxonomy of benthic foraminiferal  
127 species has been realized thanks to the Atlas of Benthic Foraminifera (Holbourn et al., 2013)  
128 and Loeblich and Tappan (1988). Scanning electronic microscope images of the most abundant  
129 species are represented in plate 1 (supplementary 1). Specimens were considered living when  
130 all chambers, except the last one, were stained. In case of doubt, notably for the miliolids, tests  
131 were broken to ensure that the staining came from internal cytoplasm.



132 Table 1. List of collected samples. Note that Cap\_CL11 was analyzed for geochemistry only  
133 and Cap\_CL6 for foraminifera only.

Core name	Site	Station code	Day	Lat. N	Long. W	Water depth (m)	Geoch.	Foram.	Indiv.	S	H'	E
755-3_CL6	Montsegur N	MS N_CL6	15.09.2020	37 17.296	32 16.524	1703	0-5 cm	0-1 cm	16	8	1,808	0,7623
755-3_CL10	Montsegur N	MS N_CL10	15.09.2020	37 17.294	32 16.524	1703	0-8 cm	0-5 cm	33	14	2,317	0,7249
755-3_CL11	Montsegur N	MS N_CL11	15.09.2020	37 17.298	32 16.522	1703	0-6 cm	0-5 cm	34	7	1,582	0,695
757-5_CL6	Capelinhos	Cap_CL6	17.09.2020	37 17.413	32 15.809	1684	NA	0-1 cm	1	1	0	1
757-5_CL11	Capelinhos	Cap_CL11	17.09.2020	37 17.384	32 15.793	1684	0-6 cm	NA	NA	NA	NA	NA
757-5_CL7	Capelinhos	Cap_CL7	17.09.2020	37 17.403	32 15.799	1684	5-7 cm	0-5 cm	3	2	0,6365	0,9449
759-7_CL11	Eiffel Tower W	ET W_CL11	21.09.2020	37 17.344	32 16.556	1697	0-5 cm	0-5 cm	NA	NA	NA	NA
759-7_CL6	Eiffel Tower W	ET W_CL6	21.09.2020	37 17.344	32 16.552	1697	0-5 cm	0-5 cm	81	20	2,525	0,6245
760-8_CL7	Eiffel Tower E	ET E_CL7	22.09.2020	37 17.343	32 16.514	1701	0-7 cm	0-5 cm	7	5	1,475	0,8743
760-8_CL6	Eiffel Tower E	ET E_CL6	22.09.2020	37 17.343	32 16.511	1701	0-5 cm	0-5 cm	83	14	2,205	0,6476
761-9_CL6	South Crystal	SC_CL6	22.09.2020	37 17.408	32 16.974	1719	0-9 cm	0-5 cm	38	11	2,025	0,6886
762-10_CL6	Montsegur	MS_CL6	24.09.2020	37 17.281	32 16.528	1702	0-4 cm	0-4 cm	1	1	0	1
762-10_CL11	Montsegur	MS_CL11	24.09.2020	37 17.281	32 16.528	1702	0-4 cm	0-4 cm	NA	NA	NA	NA
763-11_CL11	Montsegur Ref	MS Ref_CL11	24.09.2020	37 17.220	32 16.501	1712	0-8 cm	0-5 cm	58	16	2,497	0,7592
763-11_CL6	Montsegur Ref	MS Ref_CL6	24.09.2020	37 17.221	32 16.503	1712	0-8 cm	0-5 cm	101	22	2,333	0,4684

134  
135 Bulk chemical composition of each surface sediment (0-1 cm) sample was determined using a  
136 wavelength dispersive X-ray fluorescence spectrometer (BRUCKER AXS S8 Tiger) at Ifremer.  
137 Samples were ground to a powder (90% of particles < 80  $\mu$ m) using an agate pestle and mortar.  
138 Major elements and selected trace elements were analyzed on pressed pellets and fused beads  
139 (with a specific preparation for S analysis of sulfide-rich sediment; supplementary 2). After  
140 acquisition, the measured net peak intensities, corrected for inter-element effects, were  
141 converted into concentrations using calibration curves generated from analysis of certified  
142 geochemical standard powders (measured under identical analytical conditions).

143 Total organic carbon and its isotopic signature (TOC,  $\delta^{13}\text{C}_{\text{TOC}}$ ) have been measured using a  
144 LECO TruMac, after carbonate dissolution (HCl 1N) at Ifremer. Accelerator Mass  
145 Spectrometry  $^{14}\text{C}$  dating has been performed on 7 samples from two blade cores, in order to  
146 estimate sedimentation rates near the active Eiffel Tower edifice (ET E\_CL7) and at the  
147 periphery of the vent field (MS Ref\_CL6). Radiocarbon dating was carried out at the Beta



148 Analytic Radiocarbon Dating facilities in Miami, US. The age was converted into calendar  
149 years using the calibration program Calib 7.1 (Stuiver et al., 2014) with a marine reservoir age  
150 of -400 years that was incorporated within the Marine13 calibration curve (Reimer et al., 2013).  
151 Faunal and environmental statistics have been performed using the software Primer v6.0  
152 (Clarke and Warwick, 1994), for diversity indices (specific richness, Shannon and Evenness  
153 indices), principal component analysis (PCA) and matrices calculations (BioEnv). A PCA has  
154 been performed including standardized (minus average, divided by standard deviation)  
155 environmental parameters (Fe<sub>2</sub>O<sub>3</sub>, S, Cu, Ba, MnO, SiO<sub>2</sub>, CaO, TC, TOC, δ<sup>13</sup>C and grain size)  
156 and standardized living faunal descriptors (individuals, specific richness and Shannon Index  
157 values) in order to investigate the control factors of the faunal distribution. A redundancy  
158 analysis (RDA) was performed to investigate the influence of environmental variables on the  
159 distribution of dead and living most abundant taxa in the 0-1 cm layer. Dead and living  
160 organisms were pooled together in order to restrain taphonomical impacts, such as  
161 disappearance of soft-bodied foraminifera and seasonal effects and to ensure robust  
162 interpretations as rarefaction curves tend to show underestimation through living fauna  
163 (supplementary 3). Six species and two taxonomic groups were kept for the RDA analysis:  
164 *Quinqueloculina auberiana*, *Cibicides wuellerstorfi*, *Cibicides pachyderma*, *Cruciloculina*  
165 *triangulifera*, *Epistominella exigua*, *Gavelinopsis translucens*, pooled *Fissurina* species and  
166 pooled non calcareous species. RDA was performed with the R software (R core team, 2025)  
167 and the vegan package (Oksanen et al., 2001). A forward selection was implemented to select  
168 the environmental variables significantly explaining the species distribution (function ordistep  
169 of the vegan package).  
170 A correlation of environmental (Euclidean distance) and faunal (Bray-Curtis dissimilarity)  
171 matrices has been performed through the test BEST (BioEnv) to determine the main elements  
172 impacting the distribution of both fossil and living fauna on the study area (2 tests on total



173 abundances). Environmental parameters considered in the calculation were grain size, SiO<sub>2</sub>,  
174 Fe<sub>2</sub>O<sub>3</sub>, MnO, CaO, S, Ba, Cu,  $\delta^{13}\text{C}$ TOC, TOC and TC.

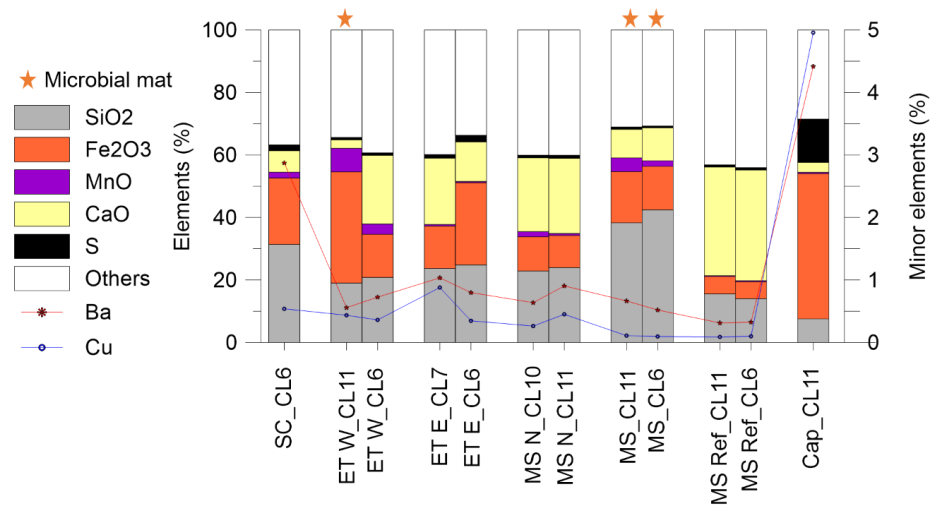
175

176 4. Results

177 4.1. Microhabitat characterization

178 Sediment microhabitats have been studied through their particulate element composition, the  
179 main elements measured in each core surface (0-1 cm) have been represented as bar charts of  
180 relative abundance (Fig. 2) and secondary elements as superposed curves.

Sediment geochemistry (0-1 cm)



181

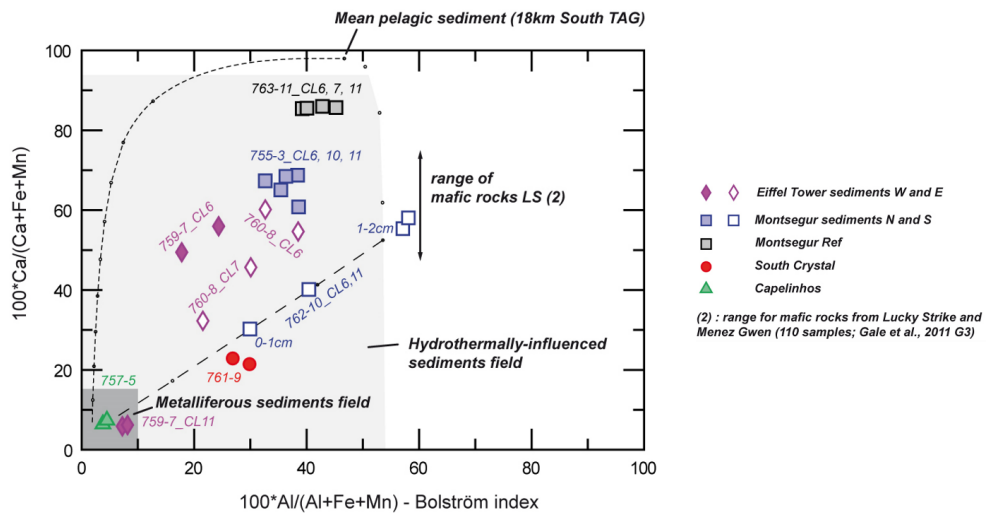
182 Fig. 2. XRF analyses of top layers (0-1 cm) of the 12 sediment cores sampled in 2020 on the  
183 Lucky Strike vent field (Mid-Atlantic Ridge). Ba and Cu are plotted as minor elements (right  
184 scale).

185

186 CaO represented the main component of stations MS N and MS Ref ranging from 24 to 35%.  
187 SiO<sub>2</sub> values ranged from 8% (station Cap\_CL6) to 42% (station MS\_CL6). Fe<sub>2</sub>O<sub>3</sub> and S were



188 the most abundant elements in station Cap\_CL6, reaching 46% and 14%, respectively. This  
 189 station also showed peaks of Ba (4.4%) and Cu (4.9%). Fe<sub>2</sub>O<sub>3</sub> (36%) and MnO (8%) were high  
 190 in station ET W\_CL6. Finally, relatively high Fe<sub>2</sub>O<sub>3</sub> (21%) and Ba (2.8%) have been measured  
 191 in station SC\_CL6. Major elements signature of surface sediments is related to mixing of  
 192 particles from three different origin (Fig. 3): (1) pure pelagic sediments (carbonate), (2) pure  
 193 metalliferous sediments (sulfides and/or oxides) and (3) mafic rocks (i.e., basalt) from the  
 194 oceanic crust.



195  
 196 Fig. 3. Bolström diagram representing the geochemical analyses of the top sediment layers (0-  
 197 1 cm) in the peripheries of four active edifices on the Lucky Strike vent field (Mid-Atlantic  
 198 Ridge).

199  
 200 Sediments from Montsegur\_Ref shows only little hydrothermal particles contribution and plot  
 201 close to the mean pelagic sediment composition. Sediments from Capelinhos and two from  
 202 Eiffel Tower W plot inside the metalliferous sediment field (Fig. 3) indicating a strong  
 203 hydrothermal influence. Sediments from Montsegur S and South Crystal plot on a mixing line  
 204 between metalliferous sediments and mafic rocks. Distribution of other sediments in Figure 3



205 indicate a variable mixture of pelagic sediments, mafic rocks fragments and metalliferous  
206 sediments.

207 Sedimentation rates have been calculated from two different sites (supplementary 4), one in the  
208 vicinity of the Eiffel Tower edifice (ET E\_CL7) and one in the south periphery of Lucky Strike  
209 (MS Ref\_CL6). These sedimentation rates showed relatively stable trends, especially for the  
210 station MS Ref\_CL6, indicating a mean value of 2.3 cm.kyr<sup>-1</sup>. At the basis of the Eiffel Tower  
211 edifice, the sedimentation rate was 4.3 cm.kyr<sup>-1</sup>.

212 Inorganic and organic carbon as well as  $\delta^{13}\text{C}$  of organic carbon have been measured on surface  
213 sediment samples (0-1 cm) and summarized in Table 2. Total carbon (TC) data showed  
214 maximal values in MS Ref stations, exceeding 7.5%. Minimum values (<1%) were obtained in  
215 the three cores targeting microbial mats (ET W\_CL11, MS\_CL6 and MS\_CL11) and in the  
216 SC\_CL6 core. Maximal total organic carbon (TOC) values were obtained in station MS  
217 N\_CL11, Cap\_CL6 and MS Ref.  $\delta^{13}\text{C}_{\text{TOC}}$  ranged from -25.4‰ (ET W\_CL11) to -22.3‰ (MS  
218 Ref\_CL11).

219 Table 2. Organic and inorganic carbon data.

Core	TC (%)	TOC (%)	TOC st. dev.	$\delta^{13}\text{C}_{\text{TOC}}$	$\delta^{13}\text{C}_{\text{TOC}}$ st. dev.
MS N_CL6	2.19	0.17	0.002	-23.40	0.01
MS N_CL10	4.68	0.22	0.012	-22.63	0.35
MS N_CL11	4.90	0.32	0.033	-23.13	0.11
Cap_CL11	1.21	0.30	0.000	-23.58	0.00
ET W_CL11	0.80	0.18	0.012	-25.35	0.91
ET W_CL6	4.43	0.23	0.007	-23.35	0.11
ET E_CL7	1.99	0.19	0.010	-25.34	0.46
ET E_CL6	4.13	0.29	0.014	-23.87	0.15
SC_CL6	0.73	0.22	0.014	-25.11	0.35
MS_CL6	0.21	0.21	0.016	-24.35	0.53
MS_CL11	0.39	0.17	0.013	-24.66	0.41
MS Ref_CL11	7.66	0.26	0.004	-22.30	0.10
MS Ref_CL6	8.02	0.27	0.002	-22.34	0.11

220

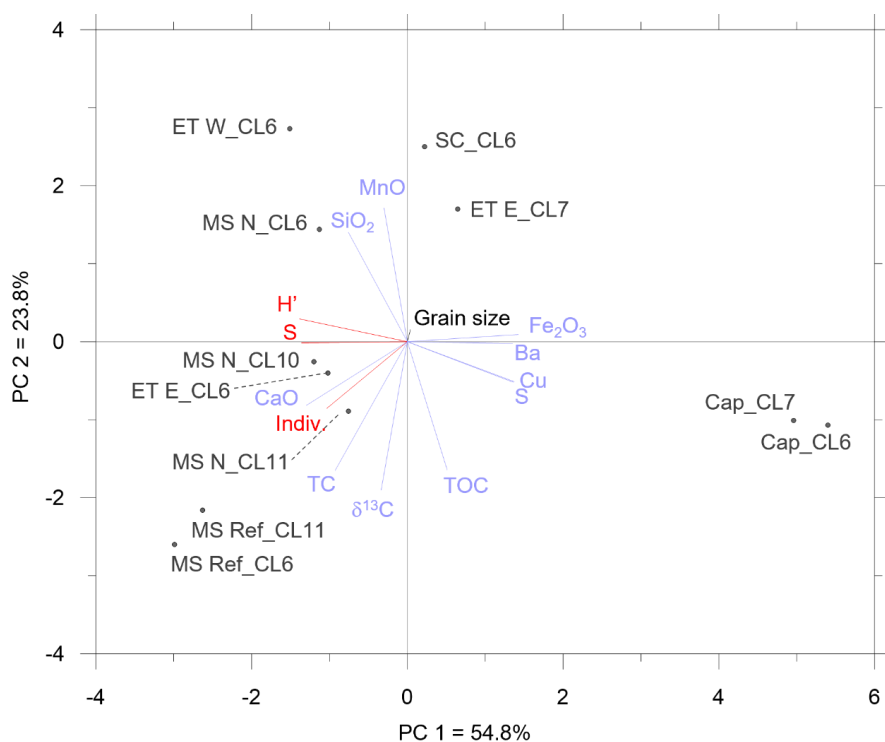


221 4.2. Foraminiferal distribution

222 In total, 54 species have been identified on the whole study area. Living individuals showed  
223 contrasted densities and diversities (Table 1) with the highest number of individuals (101) and  
224 specific richness (22) in station MS Ref\_CL6 and a minimum of 1 individual in station  
225 Cap\_CL6. Relatively high diversity characterized stations MS Ref\_CL6 and ET E\_CL6 with  
226 Shannon indexes of 2.5. The rest of the stations displayed Shannon index values ranging from  
227 0.6 to 2.3.

228 When combining both living and dead individuals, the relationship between the specific  
229 richness and the number of identified individuals showed similar trends for most of the stations  
230 indicating that more than 90% of the species are identified within the first 300 individuals of  
231 the total assemblages. Stations ET E\_CL6 and MS Ref\_CL6 showed the highest diversity with  
232 30 and 28 species for 300 individuals, respectively. A minimum of 13 species for 300  
233 individuals was observed in MS N stations. Three cores revealed the absence (or only one  
234 individual) of benthic foraminifera (MS\_CL6 and CL11 and ET W\_CL11) where microbial  
235 mats have been targeted for the sampling.

236 A PCA was conducted to investigate the environmental factors influencing living benthic  
237 foraminiferal communities (Fig. 4).



238

239 Fig. 4. Principal Component Analysis with environmental parameters in blue and biological  
240 metrics in red. H' = shannon index, S = specific richness, Indiv. = number of individuals.

241

242 The first two axes account for 78.6% of the total data variability, with PC1 explaining 54.8%  
243 and PC2 explaining 23.8% of the variance. PC1 seemed to correspond to hydrothermal inputs  
244 with positive loadings for the elements  $Fe_2O_3$ , S, Cu and Ba and slightly positive loading for  
245 TOC, while CaO displayed the most negative loading. Hence, the hydrothermal-derived  
246 elements on the PC1 particularly isolated the cores Cap\_CL7 and Cap\_CL6, representing the  
247 hydrothermal domain. SC\_CL6 and ET E\_CL7 also showed positive loading on PC1,  
248 suggesting a significant hydrothermal signal. The second axis suggested a control of the organic  
249 matter source with negative loadings of TC and  $\delta^{13}C$  and CaO. Positive loadings on the PC2  
250 were characterized by MnO and SiO<sub>2</sub>. All cores showing negative loadings for both PC1 and



251 PC2 were characterized by a pelagic sedimentation dominated by phytodetrital organic matter  
252 ( $\delta^{13}\text{C} \sim -20 \text{ ‰}$  and high CaO content), representing the reference domain with cores MS  
253 Ref\_CL11 and MS Ref\_CL6. The last domain visible on the PCA was intermediate, showing a  
254 lower contribution of elements from the pelagic sedimentation (CaO) or from hydrothermal  
255 input ( $\text{Fe}_2\text{O}_3$ , S, Cu and Ba), resulting in higher contribution of  $\text{SiO}_2$ . MnO content suggested a  
256 slight influence of hydrothermal-derived particles, probably originating from low temperature  
257 Mn-oxides precipitation. The abundance of living benthic foraminifera was well correlated with  
258 the reference domain while faunal diversity better corresponded to the intermediate domain,  
259 suggesting an influence of the source of organic matter. BioEnv statistical tests (BEST, Primer  
260 v.06) was performed on both dead and living faunal communities with environmental data  
261 (Table 3). Both tests highlighted the control of  $\text{Fe}_2\text{O}_3$  alone for the living communities and  
262  $\text{Fe}_2\text{O}_3$  with Ba for the dead ones as main control of faunal variability (Table 3), confirming the  
263 impact of hydrothermal-derived microhabitats at a regional scale.

264

265 Table 3. Statistical test BioEnv (matrices correlation).

BioEnv (living fauna). significance: 4%

Variables number	R <sup>2</sup>	Variables
1	0.664	$\text{Fe}_2\text{O}_3$
2	0.659	$\text{Fe}_2\text{O}_3$ , Ba
2	0.652	$\text{Fe}_2\text{O}_3$ , Cu
3	0.651	$\text{Fe}_2\text{O}_3$ , Ba, Cu

BioEnv (dead fauna). significance: 2%

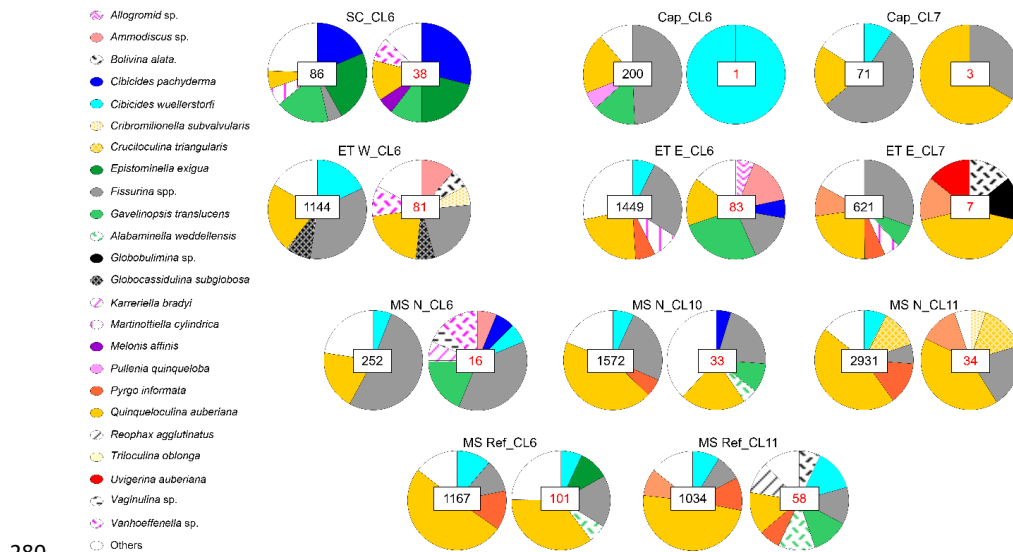
Variables number	R <sup>2</sup>	Variables
2	0.796	$\text{Fe}_2\text{O}_3$ , Ba
3	0.796	$\text{Fe}_2\text{O}_3$ , S, Ba
3	0.795	$\text{Fe}_2\text{O}_3$ , Ba, Cu
4	0.795	$\text{Fe}_2\text{O}_3$ , S, Ba, Cu

266

267



268 The whole study area was dominated by *Quinqueloculina auberiana* and *Fissurina orbignyana*  
269 (the most abundant species among the *Fissurina* genus) (Fig. 5). In the southern most station,  
270 the Miliolid order was well represented with *Q. auberiana*, *Pyrgo informata*, *Cribromiliolinella*  
271 *subvalvularis*, *Cruciloculina triangularis* and *Triloculina oblonga* as well as other calcareous  
272 species *Cibicides wuellerstorfi* and *Fissurina orbignyana*. Non-calcareous species  
273 (agglutinated and allogromids) were mainly present in intermediate stations (MS N; ET W and  
274 ET E) such as *Martinottiella cylindrica*, *Karreriella bradyi* and *Vanhoeffenella* sp. Among the  
275 most abundant species, *Gavelinopsis translucens* had its highest relative contribution in stations  
276 ET E\_CL6 and SC\_CL6, in the latter associated with *Epistominella exigua* and *Cibicides*  
277 *pachyderma*. Stations Cap\_CL6 and Cap\_CL7 were characterized by a strong dominance of  
278 *Fissurina* spp, (~50%) including all identified species from this genus (*F. orbignyana*, *F.*  
279 *annectens*, *F. foliformis*, *F. laevigata*).

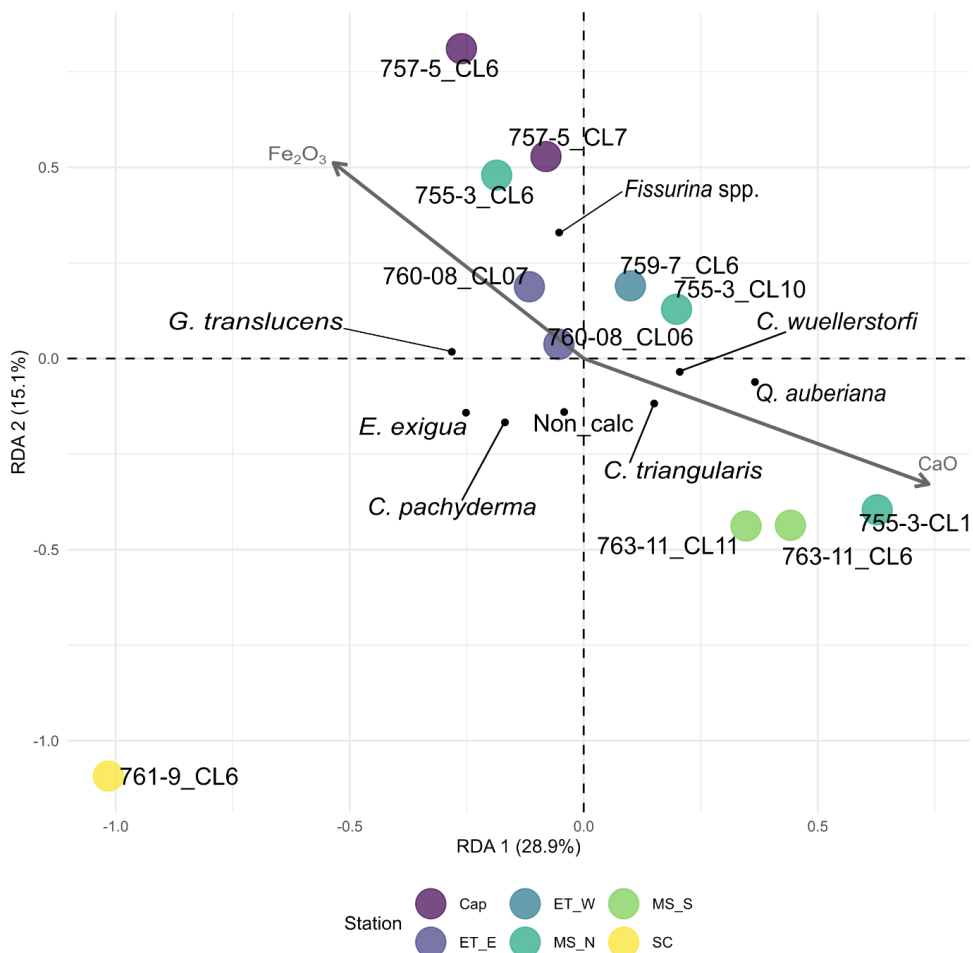


281 Fig. 5. Relative abundance (pie charts) and absolute number of individuals of the main benthic  
282 foraminiferal species (e.g., representing >5%) of the total abundance with dead communities  
283 represented on the left (black numbers) and living communities on the right (red numbers).

284



285 The RDA performed on the main species distribution selected only CaO and Fe<sub>2</sub>O<sub>3</sub> ( $p < 0.05$ )  
286 when implementing the forward selection on environmental variables (Fig. 6).



287  
288 Fig. 6. Redundancy Analysis of the main benthic foraminiferal species (>5% of the total  
289 abundance) of the Lucky Strike vent field based on dead + living communities and  
290 environmental parameters of the top sediment layers (0-1 cm).

291

292 The first two axes represent together 44% of the data variability. Main distinctions are visible  
293 along the pelagic to hydrothermal gradient with *Q. auberiana* dominant in the reference cores  
294 on the bottom right quadrant of the RDA, associated with pelagic sedimentation (correlated to



295 CaO) while *Fissurina* spp. were dominant in cores Cap\_CL6 and Cap\_CL7, in the most intense  
296 hydrothermal domain in the top left quadrant (correlated to Fe<sub>2</sub>O<sub>3</sub>). Cores in other venting  
297 locations are intermediate, with an exception with the South Crystal's core, showing a distinct  
298 pattern with the dominance of *E. exigua* and *C. pachyderma* species.

299

300 5. Discussion

301 5.1. Environmental control on faunal distribution

302 The Lucky Strike vent field developed on the summit of a large volcano (Ondréas et al., 2009)  
303 mainly composed of enriched mid-ocean ridge basalt (EMORB) characterized by high barium  
304 contents compared to normal MORB. This geological context allowed the enrichment in Fe and  
305 H<sub>2</sub>S in the area as well as Cu, S, Zn and Ba in the close vicinity of the black smokers (Cotte et  
306 al., 2020). Our results confirm a sedimentary content enriched in these elements at close  
307 periphery of active edifices, while further periphery mainly represents phytodetritic influence.  
308 The contribution of hydrothermal-derived material close to Eiffel Tower edifice hence  
309 represents about 2.0 cm kyr<sup>-1</sup> that corresponds to half of the sediment material. The elements  
310 measured in Capelinhos and South Crystal suggest an important geochemical maturation  
311 originating from the hydrothermally-derived metalliferous sediments, or more likely in  
312 Capelinhos from vestiges of inactive chimneys covering the sediment, as suggested by the pore  
313 water dissolved metals profiles (supplementary 5) thus implying a different potential impact on  
314 faunal distribution.

315 Inorganic carbon data appeared correlated with CaO content, mainly derived from the presence  
316 of planktonic foraminifera that were the most abundant in MS Ref stations according to visual  
317 stereoscopic microscope observations. Stable isotopic signature of carbon in these stations  
318 demonstrated a classical marine signal of phytodetritic material (Meyers, 1994). More depleted

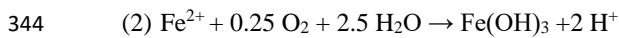


319  $\delta^{13}\text{C}$  of the sedimentary organic carbon measured in the vicinity of hydrothermal edifices Eiffel  
320 Tower, Capelinhos and South Crystal and within microbial mats suggested a microbial  $^{13}\text{C}$   
321 depletion. Hence, the benthic foraminiferal food source varied from exclusive phytodetritic  
322 material in the MS Ref stations to mixed pelagic and microbial carbon sources in periphery  
323 stations, and exclusive microbial source in mats.

324 Even though statistical tests on environmental control on fauna indicate a first variance  
325 explanation based on sedimentary content (i.e., Fe, Ba and CaO), these parameters showed  
326 significant autocorrelations with TOC and  $\delta^{13}\text{C}$  of the organic carbon, suggesting that  
327 hydrothermal-derived material is strongly linked with the quantity and source of organic matter  
328 available for foraminiferal communities and should be considered for faunal interpretation.  
329 Additionally, microbial biofilms were not included in statistical tests because of the absence of  
330 fauna, being nevertheless key for distribution understanding.

### 331 5.2. A toxic microbial biofilm for foraminifera?

332 The abundance of both living and fossil benthic foraminifera suggested a main control by  
333 organic carbon content in the sediment that was not directly connected to the influence of  
334 venting activity. In particular, the cores collected on the zetaproteobacteria microbial mats  
335 (MS\_CL11, MS\_CL6 and ET\_W\_CL11) revealed the absence of foraminifera. The visual  
336 observations of sediment samples pointed out the absence of all carbonated material, such as  
337 planktonic foraminifera, resulting in a very low total carbon and carbonate content (Table 2).  
338 These stalk-forming iron-oxidizing bacteria are known to produce flocculent iron oxide mats,  
339 which can be meters thick and cover hundreds of square meters (Emerson and Moyer, 2002).  
340 While oxidizing iron, they use Fe(II) and oxygen producing Fe(III) (eq. 1), that also occurs  
341 through abiotic reaction that almost directly results in the production of iron oxyhydroxides at  
342 circumneutral pH through the reaction (eq. 2) (Emerson et al., 2010).



345 In order to limit the precipitation of Fe(III); as well as produced by the abiotic iron oxidation in  
346 iron oxyhydroxides; they excrete acidic polysaccharids that acidify (to pH = 6) their  
347 microhabitat outside their cells in order to bind the Fe(III) and prevent its precipitation in  
348 minerals (Cohen, 2020). Hence, zetaproteobacteria biofilms may significantly decrease the  
349 microenvironmental pH in their mats, resulting in the dissolution of fossil planktonic  
350 foraminifera and preventing benthic foraminiferal colonization in surrounding sediments.  
351 These microbial communities are abundant on basaltic-rich substrates at the Lucky Strike vent  
352 field where they use the structural Fe(II) from the basaltic glass (Henri et al., 2016). Whether  
353 the absence of benthic foraminifera is explained by the presence of the microbial mats  
354 themselves (competition or lack of sediment substratum) or by the pH of the biofilm is unclear.  
355 However, the absence of all carbonated tests (planktonic foraminifera, ostracods, bivalves,  
356 gastropods) in these cores, combined with a very low inorganic carbon content in the three  
357 “microbial mat” cores further support the hypothesis of a dissolution of all carbonates in the  
358 mat. The organic carbon source there, might be limited to the microbial community itself,  
359 without pelagic contribution. Considering the sedimentation rate (2.3 cm kyr.<sup>-1</sup>) and the  
360 carbonate content in the pelagic end-member, this dissolution would result in a rate of 0.5  
361 mg(CaCO<sub>3</sub>).cm<sup>-3</sup>.yr<sup>-1</sup>, that might have a significant impact on regional carbon budget  
362 considering the area covered by these mats.

363 5.3. The pelagic end-member

364 In the control stations (MS Ref), the organic carbon content showed its higher values in the  
365 study area, though it remained low compared to classical deep-sea environments (e.g.,  
366 Dessandier et al., 2016; 2019; Krüger et al., 2025). Notably, these stations were characterized  
367 by the most abundant and diverse communities of both fossil and living benthic foraminifera.



368 The presence of miliolid species and *C. wuellerstorfi*, characterizing these stations, suggests a  
369 pre-degraded organic matter, which might correspond to phytodetritic deposits from the last  
370 spring. The main difference in the assemblages of benthic foraminifera between the reference  
371 and intermediate stations corresponds to the decrease of miliolid relative abundance with  
372 increasing proximity to the vents. This may be explained by the calcification strategy of this  
373 order that precipitate a shell with high Mg/Ca carbonate, hence necessitating an elevated pH in  
374 comparison with that of the surrounding water (de Nooijer et al., 2009). Since the pH in  
375 sediments and water at Lucky Strike drastically decreases from the periphery to the edifices  
376 (Sarradin et al., 1999), the energetic effort to precipitate these shells may be limiting. These  
377 results are in contradiction with a recent study conducted at the Rainbow vent field (Krüger et  
378 al., 2025) where miliolids have been observed in the closest relationship with hydrothermal  
379 plume. This could be explained by both a different geochemical context in Rainbow vent field  
380 and a different sampling strategy, with cores collected between 200 m and 41 km of distance to  
381 vents in Krüger et al. (2025) while all cores were distant from less than 50 m to chimneys in  
382 the present study (except for MS\_Ref stations). Some *C. wuellerstorfi* individuals observed in  
383 the present study morphologically resembles *Cibicides lobatulus* taxon, conforming the shape  
384 of their test to the substrate where they are attached. Recently, it has been demonstrated that  
385 genetically identified *C. wuellerstorfi* flourishing on hard substrata present different  
386 morphologies from “classical” *C. wuellerstorfi* to ecophenotype *C. wuellerstorfi* var. *lobatulus*  
387 (Burkett et al., 2020). These authors proposed that both the substratum and microbial  
388 colonization influence the distribution of *Cibicides* species. *Cibicides pachyderma* is a  
389 facultative epifaunal species that preferentially lives as an infaunal dweller in moderate carbon  
390 flux areas, able to cover parts of its test by aggregates or algae in low pH environments  
391 (Wollenburg et al., 2018). Hence, this species may replace *C. wuellerstorfi* in environments  
392 characterized by harsher environmental conditions, such as slightly lower pH.



393 5.4. Intermediate habitats, a pool of diversity

394 The stations in the vicinity of hydrothermal edifices Eiffel Tower and Montsegur harbored  
395 abundant and diverse fossil fauna while the living community remained less developed.

396 Interestingly, the faunal diversity of the living community around Eiffel Tower appeared  
397 relatively high, showing abundant non-calcareous species (e.g., *Vanhoeffela* sp., *Reophax*  
398 *agglutinatus*, *Martinorinella cylindrica* and allogromid sp.) and *Globocassidulina subglobosa*  
399 that were rare in the rest of the stations. Monothalamids may be present in a greater extent due  
400 to harder substrata where they can attach their test, preferentially to most of the calcareous taxa.

401 Their occurrence at Lucky Strike was however limited, in comparison with other deep-sea  
402 environments (e.g., Koho et al., 2007) potentially because of low pH microenvironments. As  
403 observed for agglutinated species in cold seeps (e.g., Dessandier et al., 2019), these species  
404 might not easily tolerate the environmental conditions derived from hydrothermal venting.

405 Nevertheless, several of these species represent pioneer recolonizers following the end of  
406 venting or sediment disturbance (Kitazato, 1995; Panieri et al., 2005) and may flourish on  
407 inactive chimneys. The cores collected in sediments enriched in iron and sulfur (Capelinhos)  
408 displayed generally lower dead faunal abundances than those from the intermediate stations.

409 Interestingly, South Crystal site, that is more a mix of basalt and metalliferous sediment, is  
410 characterized by a substantial living individuals' density and a slightly different faunal  
411 distribution, with *G. translucens*, *E. exigua* and *C. pachyderma* as the most abundant species.

412 This assemblage highlights a potential fresher organic material than in the other stations that  
413 may be linked to a higher microbial productivity, triggered by the high content in iron and  
414 sulfur. Sen Gupta and Aharon (1994) observed *G. translucens* as a dominant taxon in a bathyal  
415 vent community of the Gulf of Mexico, associated with bacterial (*Beggiatoa*) mats and tolerant  
416 to anoxic conditions and high H<sub>2</sub>S concentrations in sediments. Most of the deep-sea species  
417 may experience dormancy phases during periods of starvation and are likely able to switch to a



418 biologically active phase when phytodetritus pulses reach the seafloor (Gooday and Rathburn,  
419 1999), with a response that differs at daily to seasonal scales. In bathyal north Atlantic  
420 environment, *Quinqueloculina* sp. has been observed as dominant in late summer, after the  
421 degradation of fresh phytodetritic material, replacing opportunistic species (e.g., *Alabaminella*  
422 *weddellensis*, *E. exigua*) at the sediment water interface, after a probable migration up from a  
423 shallow infaunal microhabitat (Gooday and Rathburn, 1999). This phenomenon could explain  
424 the dominance of *Q. auberiana* in our study area sampled in September while opportunistic  
425 species (*G. translucens* and *E. exigua* and *A. weddellensis*) are restricted to sediments harboring  
426 additional food sources represented by microbial communities. *Epistominella exigua* and *A.*  
427 *weddellensis* represent the most common species in the deep-sea Atlantic Ocean in the >63 µm  
428 size fraction (Sun et al., 2006). These opportunistic species flourish whenever suitable food  
429 sources -such as phytoplankton or microorganisms (Turley et al., 1993)- become available  
430 (Gooday, 1988).

431 5.5. Capelinhos, the sulfide-rich metalliferous microhabitat  
432 This living community was absent in Capelinhos where the very high content in hydrothermal-  
433 derived elements have probably directly or indirectly restrained foraminiferal growth.  
434 However, considering the elevated number of fossils in these two stations, it is clear that the  
435 microenvironment is not preventing colonization by benthic foraminifera as observed in the  
436 zetaproteobacterial mats. An equilibrium between the source of energy that promotes microbial  
437 communities and the more classical marine conditions represented in the reference stations  
438 seems to be necessary for the development of these opportunistic species that can thrive in  
439 sediments slightly impacted by venting. Surprisingly, a strong dominance of *Fissurina*  
440 *orbignyana* has been observed in the two Capelinhos stations as well as in one of the  
441 intermediate stations around Montsegur edifice. Very little is known about the ecology of the  
442 genus *Fissurina*, often observed in deep-sea environments, but never abundant enough to



443 decipher its ecology. Its occurrence in both the intermediate and extreme environments (i.e.,  
444 rich in Fe, S and Cu) suggest a wide range of tolerance for these single chambered specimens.  
445 Even though Capelinhos edifice lies in a different chemical domain than other edifices of the  
446 Lucky Strike vent field (Chavagnac et al. 2018), with the most enriched metal content (Cotte et  
447 al., 2020), we cannot exclude that the fossils observed of *Fissurina* species come from a period  
448 of a less intense vent activity. Alternatively, the more intense hydrothermal impact observed in  
449 this particular core may reflect a different source of particles that could originate from  
450 dismantled past chimneys, hence representing harsher environment than diffusion of metal from  
451 particles deposited through the hydrothermal plume. Further investigations on the tolerance of  
452 these species for high metallic content may be of interest in the future to better understand the  
453 ecology of this group.

454

455 6. Conclusions

456 Extensive symbiotic relationships between microorganisms and macrofauna lead to a bypass of  
457 meiofauna as major contributors in the vent trophic network. This limited role in energy transfer  
458 may explain why meiofauna -especially foraminifera- has received relatively little attention in  
459 these ecosystems. However, benthic foraminifera represent an essential chain of the deep-sea  
460 food web, making a link between phytoplanktonic and microbial communities on which they  
461 feed and a substantial number of predators from the metazoans feeding on foraminifera. In  
462 hydrothermal systems, the environmental conditions represent a challenge for these organisms  
463 to thrive (e.g., low pH, high H<sub>2</sub>S content, hard substrates and in particular low organic carbon  
464 content), hence leading to a crucial role of microbial communities as an additional food source  
465 but also by the role they have in changing the environment (e.g., consuming H<sub>2</sub>S).



466 Our results demonstrated that the microbial food source allowed benthic foraminiferal  
467 opportunistic species to flourish in the direct vicinity to active chimneys where the elements  
468 present in the sediment (Fe, S) originated high microbial content. In the reference cores, the  
469 foraminiferal community showed adaptation for more refractory organic matter, which is  
470 partially explained by the period of sampling. Directly opposed to this trend, the establishment  
471 of biofilm from Zetaproteobacteria seems to trigger the dissolution of all carbonated shells. The  
472 absence of agglutinated or organic-walled specimens in these mats even revealed a toxic  
473 environment for all benthic foraminifera. This observation questions the role of these extended  
474 microbial mats in the carbon fluxes in hydrothermal vent systems, with the dissolution of  
475 foraminiferal tests that might export carbon from the sediment to the water column. The reasons  
476 for the establishment of mats of Zetaproteobacteria remains uncertain (Emerson et al., 2010),  
477 and no direct link can be made when focusing on the iron content in the sediment. This  
478 observation points out the extreme heterogeneity of the hydrothermal-derived microhabitats  
479 that affects the regional biodiversity where benthic foraminifera represent a powerful bio-  
480 indicator.

481 In the absence of symbiosis between microbes and macrofauna that occurs only in active  
482 hydrothermal vents, benthic foraminifera may represent a key trophic chain for the inactive  
483 systems. The intermediate stations observed in this study represent good analogues for inactive  
484 hydrothermal chimneys inhabiting microbial communities that use reduced elements  
485 accumulated in the sediments. There, benthic foraminiferal communities showed their highest  
486 diversities. These systems are nowadays under the scope of the society for economic interests  
487 in metalliferous sediment associated to sulfides deposits. There, the local biodiversity may be  
488 clearly impacted by removal the life conditions of benthic foraminifera. Hence, a good  
489 knowledge on benthic foraminiferal ecology from these environments, close to active vents, in



490 the periphery and on inactive chimneys appears essential to prevent any damage in the deep-  
491 sea biodiversity.

492

493 Acknowledgements

494 The authors would like to thank the captain and the crew of the *R/V Pourquoi Pas?* and the  
495 chief scientist P.M. Sarradin. This work was supported by ISblue project, Interdisciplinary  
496 graduate school for the blue planet (ANR-17-EURE-0015) and co-funded by a grant from the  
497 French government under the program "Investissements d'Avenir", and by a grant from the  
498 Regional Council of Brittany (SAD programme). We thank J.H. Ogor, M. Hubert, Y. Germain  
499 and N. Gayet for their technical help in data acquisition.

500

501 References

502 Alfaro-Lucas, J.M., Pradillon, F., Zeppilli, D., Michel, L.N., Martinez-Arbizu, P., Tanaka, H.,  
503 Foviaux, M., Sarrazin, J., 2020. High environmental stress and productivity increase functional  
504 diversity along a deep-sea hydrothermal vent gradient. *Ecology* 101(11), e031144.

505 Astorch-Cardona, A., Odin, G. P., Chavagnac, V., Dolla, A., Gaussier, H., & Rommevaux, C.,  
506 2024. Linking Zetaproteobacterial diversity and substratum type in iron-rich microbial mats  
507 from the Lucky Strike hydrothermal field (EMSO-Azores observatory). *Applied and*  
508 *Environmental Microbiology*, 90(2), e02041-23.

509 Burkett, A.M., Rathburn, A., Elena Pérez, M., Martin, J.B., 2018. Influences of thermal and  
510 fluid characteristics of methane and hydrothermal seeps on the stable oxygen isotopes of living  
511 benthic foraminifera. *Marine and Petroleum Geology* 93, 344-355.

512 Burkett, A., Rathburn, A., Pratt, R.B., Holzmann, M., 2020. Insights into the ecology of  
513 epibenthic calcareous foraminifera from a colonization study at 4000 m (Station M) in the NE  
514 Pacific Ocean. *Deep Sea Research II: Topical Studies in Oceanography* 173, 104709.



515 Childress, J.J., and Fisher, C.R., 1992. The biology of hydrothermal vent animals: physiology,  
516 bio-chemistry and autotrophic symbioses. *Oceanography and Marine Biology* 30:337–441

517 Cohen, 2020. The Ecophysiology of Iron-Oxidizing Zetaproteobacteria: Microbe-Mineral  
518 Interactions, Transcriptomic Responses, and Biomineralization. PhD Thesis

519 Cotte, L., Chavagnac, V., Pelleter, E., Laës-Huon, A., Cathalot, C., Dulaquais, G., Riso, R.D.,  
520 Sarradin, P.-M., Waeles, M., 2020. Metal partitioning after in situ filtration at deep-sea vents  
521 of the Lucky Strike hydrothermal field (EMSO-Azores, Mid-Atlantic Ridge, 37°N). *Deep Sea*  
522 *Research I: Oceanographic Research Papers* 157, 103204.

523 de Nooijer, L., Toyofuku, T., Kitazato, H., 2009. Foraminifera promote calcification by  
524 elevating their intracellular pH. *Proceedings of the National Academy of Sciences of the United*  
525 *States of America* 106 (36), 15374-15378.

526 Desbruyeres, D., Biscoito, M., Caprais, J.-C., Colaço, A., Comtet, T., Crassous, P., Fouquet,  
527 Y., Khripounoff, A., Le Bris, N., Olu, K., Riso, R., Sarradin, P.-M., Vangriesheim, A., 2001.  
528 Variations in deep-sea hydrothermal vent communities on the Mid-Atlantic Ridge near the  
529 Azores plateau. *Deep Sea Research I: Oceanographic Research Papers* 48 (5), 1325-1346.

530 Dessandier, P.-A., Bonnin, J., Kim, J.-H., Bichon, S., Deflandre, B., Grémare, A., Sinninghe  
531 Damsté, J.S., 2016. Impact of organic matter source and quality on living benthic foraminiferal  
532 distribution on a river-dominated continental margin: a study of the Portuguese margin. *Journal*  
533 *of Geophysical Research, Biogeosciences* 121, 1689–1714.

534 Dessandier, P.-A., Borrelli, C., Kalenitchenko, D., Panieri, G., 2019. Benthic foraminifera in  
535 Arctic methane hydrate bearing sediments. *Frontier in Marine Science* 6:765.  
536 <https://doi.org/10.3389/fmars.2019.00765>

537 Emerson, D., and Moyer, C.L., 2002. Neutrophilic Fe-Oxidizing Bacteria Are Abundant at the  
538 Loihi Seamount Hydrothermal Vents and Play a Major Role in Fe Oxide Deposition. *Applied*  
539 *and Environmental Microbiology* 68 (6), 3085-3093.

540 Fisher, C., Takai, K., Le Bris, N., 2007. Hydrothermal vent ecosystems. *Oceanography* 20: 14-  
541 23

542 Fouquet, Y., Ondréas, H., Charlou, J.-L., Donval, J.-P., Radford-Knoery, J., Costa, I., Lourenço,  
543 N., Tivey, M.K., 1995. Atlantic lava lakes and hot vents. *Nature* 377, 201.



544 Gooday, A.J., 1988. A response by benthic foraminifera to phytodetritus deposition in the deep  
545 sea. *Nature* 332, 70–73

546 Gooday, A.J., 1994. The biology of deep-sea foraminifera: A review of some advances and  
547 their applications in paleoceanography. *Palaios* 9, 14-31.

548 Gooday, A.J., and Rathburn, A., 1999. Temporal variability in living deep-sea benthic  
549 foraminifera: a review. *Earth-Science Reviews* 46 (1-4), 187-212.

550 Henri, P.A., Rommevaux-Jestin, C., Lesongeur, F., Mumford, A., Emerson, D., Godfroy, A.,  
551 Ménez, B., 2016. Structural Iron (II) of Basaltic Glass as an Energy Source for  
552 Zetaproteobacteria in an Abyssal Plain Environment, Off the Mid Atlantic Ridge. *Frontiers in*  
553 *Microbiology*. <https://doi.org/10.3389/fmicb.2015.01518>

554 Hollander D.J., Smith M.A., 2001. Microbially mediated carbon cycling as a control on the  
555 d13C of sedimentary carbon in eutrophic Lake Mendota (USA): new models for interpreting  
556 isotopic excursions in the sedimentary record. *Geochim Cosmochim Acta* 65, 4321-4377.

557 Husson, B., Sarradin, P.M., Zeppilli, D., Sarrazin, J., 2017. Picturing thermal niches and  
558 biomass of hydrothermal vent species. *Deep-Sea Res. II Top. Stud. Oceanogr.* 137, 6–25.  
559 <https://doi.org/10.1016/j.dsr2.2016.05.028>.

560 Jonasson, K.E., Schröder-Adams, C.J., Patterson, R.T., 1995. Benthic foraminiferal distribution  
561 at Middle Valley, Juan de Fuca Ridge, a northeast Pacific hydrothermal venting site. *Marine*  
562 *Micropaleontology* 25 (2-3), 151-167.

563 Jorissen, F.J., de Stigter, H.C., Widmark, J.G., 1995. A conceptual model explaining benthic  
564 foraminiferal microhabitats. *Marine Micropaleontology* 26, 3–15.

565 Khripounoff, A., Comtet, T., Vangriesheim, A., Crassous, P., 2000. Near-bottom biological and  
566 mineral particle flux in the Lucky Strike hydrothermal vent area (Mid-Atlantic Ridge). *Journal*  
567 *of Marine Systems* 25 (2), 101-118.

568 Kitazato, H., 1995. Recolonization by deep-sea benthic foraminifera: possible substrate  
569 preferences. *Marine Micropaleontology* 26 (1-4), 65-74.

570 Koho, K.A., Kouwenhoven, T.J., de Stigter, H.C., van der Zwaan, G.J., 2007. Benthic  
571 foraminifera in the Nazaré Canyon, Portuguese continental margin: Sedimentary environments  
572 and disturbance. *Marine Micropaleontology* 66, 27-51.



573 Krüger, H., Schmiedl, G., Steiner, Z., Zhang, Z., Achterberg, E. P., & Glock, N., 2025. Change  
574 in biodiversity and abundance of benthic foraminifera with distance from the Rainbow  
575 hydrothermal vent field, Mid-Atlantic Ridge. *Journal of Micropalaeontology*, 44(2), 193-211.

576 Langmuir, C., Humphris, S., Fornari, D., Van Dover, C., Von Damn, K., Tivey, M.K.,  
577 Colodner, D., Charlou, J.-L., Desonie, D., Wilson, C., Fouquet, Y., Klinkhammer, G., Bougault,  
578 H., 1997. Hydrothermal vents near a mantle hot spot: the Lucky Strike vent field at 37°N on  
579 the Mid-Atlantic Ridge. *Earth and Planetary Science Letters* 148 (1-2), 69-91.

580 Matabos, M., Cannat, M., Ballu, V., Barreyre, T., Blandin, J., Castillo, A., ... & Sarradin, P. M.,  
581 2025. The EMSO-Azores deep-sea observatory: 15 years of multidisciplinary studies of the  
582 lucky strike hydrothermal system, from sub-seafloor to the water column. *Journal of Sea*  
583 *Research*, 102625.

584 Meyers, P.A., 1994. Preservation of elemental and isotopic source identification of sedimentary  
585 organic matter. *Chemical Geology* 114, 289-302.

586 Molina-Cruz, A., and Ayala-Lopez, A., 1988. Influence of the hydrothermal vents on the  
587 distribution of benthic foraminifera from the Guaymas Basin, Mexico. *Geo-Marine Letters* 8,  
588 49-56.

589 Oksanen, J., Simpson, G. L., Blanchet, F. G., Kindt, R., Legendre, P., Minchin, P. R., ... &  
590 Weedon, J. (2001). Vegan: community ecology package.

591 Ondréas, H., Cannat, M., Fouquet, Y., Normand, A., Sarradin, P.-M., Sarrazin, J., 2009. Recent  
592 volcanic events and the distribution of hydrothermal venting at the Lucky Strike hydrothermal  
593 field, Mid-Atlantic Ridge. *Geochemistry, Geophysics, Geosystems* 10 (2).  
594 <https://doi.org/10.1029/2008GC002171>

595 Panieri, G., 2005. Benthic foraminifera associated with a hydrocarbon seep in the Rockall  
596 Trough (NE Atlantic). *Geobios* 38, 247–255.

597 Pelleter, E., Fouquet, Y., Etoubleau, J., Cheron, S., Labanieh, S., Josso, P., Bollinger, C.,  
598 Langlade, J., 2017. Ni-Cu-Co-rich hydrothermal manganese mineralization in the Wallis and  
599 Futuna back-arc environment (SW Pacific). *Ore Geology Reviews* 87, 126-146.

600 R Core Team (2025). R: A language and environment for statistical computing. R Foundation  
601 for Statistical Computing, Vienna, Austria. <https://www.R-project.org/>.



602 Reimer, P.J., et al., 2013. Intcal13 and Marine13 radiocarbon age calibration curves 0-50,000  
603 years cal bp. *Radiocarbon* 55 (4), 1869e1887.

604 Sarradin, P.-M., Caprais, J.-C., Riso, R., Kérouel, R., Aminot, A., 1999. Chemical environment  
605 of the hydrothermal mussel communities in the Lucky Strike and Menez Gwen vent fields, Mid  
606 Atlantic Ridge. *Cahiers de Biologie Marine* 40, 93-104

607 Sarradin, P.-M., M. Waeles, S. Bernagout, C. Gall, J. Sarrazin, and R. Riso. 2009. Speciation  
608 of dissolved copper within an active hydrothermal edifice on the Lucky Strike vent field (MAR,  
609 37°N). *Science of the Total Environment* 407:869–878.

610 Sarrazin, J., P. Legendre, F. de Busserolles, M.-C. Fabri, K. Guilini, V. N. Ivanenko, M.  
611 Morineaux, A. Vanreusel, and P.-M. Sarradin. 2015. Biodiversity patterns, environmental  
612 drivers and indicator species on a high-temperature hydrothermal edifice, Mid-Atlantic Ridge.  
613 *Deep Sea Research Part II: Topical Studies in Oceanography* 121:177–192.

614 Sarrazin, J., Portail, M., Legrand, E., Cathalot, C., Laes, A., Lahaye, N., Husson, B., 2020.  
615 Endogenous versus exogenous factors: what matters for vent mussel communities? *Deep-Sea  
616 Res. I Oceanogr. Res. Pap.* 160, 103260. <https://doi.org/10.1016/j.dsr.2020.103260>.

617 Schmidt, C., Vuillemin, R., Le Gall, C., Gaill, F., & Le Bris, N., 2008. Geochemical energy  
618 sources for microbial primary production in the environment of hydrothermal vent shrimps.  
619 *Marine Chemistry*, 108(1-2), 18-31.

620 Sen Gupta, B.K., Aharon, P., 1994. Benthic foraminifera of bathyal hydrocarbon vents of the  
621 Gulf of Mexico: initial report on communities and stable isotopes. *Geo-Marine Letters* 14, 88–  
622 96.

623 Stuiver, M., Reimer, P.J., Reimer, R., 2014. CALIB radiocarbon calibration execute, version  
624 7.0.html. Available online at: <http://calib.qub.ac.uk/calib/>.

625 Sun, X., Corliss, B., Brown, C.W., Showers, W.J., 2006. The effect of primary productivity and  
626 seasonality on the distribution of deep-sea benthic foraminifera in the North Atlantic. *Deep Sea  
627 Research Part I: Oceanographic Research Papers* 53 (1), 28-47

628 Turley, C.M., Gooday, A.J., Green, J.C., 1993. Maintenance of abyssal benthic foraminifera  
629 under high pressure and low temperature: some preliminary results. *Deep Sea Research Part I:  
630 Oceanographic Research Papers* 40 (4), 643-652



631 Van Dover, C.L., 1995. Ecology of Mid-Atlantic Ridge hydrothermal vents. In: Parson, L.M.,  
632 Walker, C.L., Dixon, D.R. (Eds.), *Hydrothermal Vents and Processes* 87. The Geological  
633 Society of London Special Publication 257–294.  
634 Van Dover et al., 1996

635 Wollenburg, J.E., Zittler, Z.M., Bijma, J., 2018. Insight into deep-sea life—Cibicidoides  
636 pachyderma substrate and pH-dependent behaviour following disturbance. *Deep Sea Research*  
637 Part I: *Oceanographic Research Papers* 138, 34–45

638

639 Conflicts of Interest  
640 The authors declare no conflicts of interest.

641

642 Data Availability Statement  
643 All data have been provided as supplementary material

644

645 Authors contribution  
646 PAD designed the experiments, identified benthic foraminifera and analyzed the data. GP and  
647 JS supervised the project. RL contributed to statistical analyses and figures. EP, AB and SC  
648 analyzed and interpreted the geological data. AB and SF contributed to biological sampling and  
649 samples processing. All authors revised the manuscript.

650